JACS
JOURNAL OF THE AMERICAN CHEMICAL SOCIETY

Communication

pubs.acs.org/JACS

Measurement of Silver–π Interactions in Solution Using Molecular Torsion Balances

Josef M. Maier, Ping Li, Jungwun Hwang, Mark D. Smith, and Ken D. Shimizu*

Department of Chemistry and Biochemistry, University of South Carolina, Columbia, South Carolina 29208, United States

Supporting Information

ABSTRACT: A new series of molecular torsion balances were designed to measure the strength of individual Ag–π interactions in solution for an Ag(I) coordinated to a pyridine nitrogen. The formation of a well-defined intramolecular Ag–π interaction in these model systems was verified by X-ray crystallography and ^{1}H NMR. The strength of the intramolecular Ag–π interaction in solution was found to be stabilizing in nature and quantified to be −1.34 to −2.63 kcal/mol using a double mutant cycle analysis. The Ag–π interaction was also found to be very sensitive to changes in geometry or solvent environment.

Metal–π interactions[1] are attractive interactions between metal atoms and aromatic surfaces that play an important role in biological processes, polymer/materials design, host–guest complexes, and catalysis.[2] One of the most widely utilized metal–π interactions is the Ag–π interaction.[3] These interactions have found applications in catalysis,[4] electrospray mass-spectrometry,[5] molecular recognition,[6] and polymer/materials design.[7] Despite the utility of Ag–π interactions, a better understanding of the individual interaction strengths and stability trends is still needed to guide the rational design of new materials and applications that utilize this interaction. Individual Ag–π interactions are weak, making them difficult to experimentally study and measure. Accordingly, studies in solution have focused on systems that form multiple Ag–π interactions making it difficult to estimate the individual interaction energies.[8] Solid-state X-ray crystallographic analyses have provided information on the length and geometry of the interaction but this method only provides indirect estimates of the interaction energies.[9] Finally, computational methods have been employed to study Ag–π interactions. However, these methods tend to overestimate the strengths of cation–π interactions due to the lack of discrete solvent effects.[10] Therefore, the goal of this study was to experimentally measure the strength of individual Ag–π interactions in solution utilizing a small molecule model system, which could flip between two conformational states (Scheme 1).

Molecular torsion balances[11] **1**–**2** were designed to measure the stabilizing energy of a single intramolecular Ag(I)–π interaction from its influence on the *folded*–*unfolded* conformational equilibrium. The mode of action of **1** and **2** is similar to the dynamic systems developed by Rathore and Habata that used Ag–π interactions to control conformational equilibrium and shape of the molecules.[8a,d] We have previously demonstrated the sensitivity and versatility of the dynamic *N*-arylimide bicyclic framework in **1** and **2** to study other weak noncovalent interactions of aromatic surfaces such as CH–π,[12] CD–π,[13] cation–π,[14] and π–π interactions.[15] In this study, the pyridine nitrogen of the *N*-aryl rotor was designed to coordinate an Ag(I) ion and position it over the benzene shelf in the *folded* conformer, forming an intramolecular Ag–π interaction. Thus, the relative strengths of the intramolecular Ag–π interactions could be measured by monitoring the shifts in the *folded*–*unfolded* equilibrium in the absence and presence of Ag(I). The absolute Ag–π interaction energies could also be isolated by comparison of the folding energies of **1** or **2** with control balance **3**, which lacks a benzene π-shelf and thus cannot form an intramolecular Ag–π interaction.

Scheme 1[a]

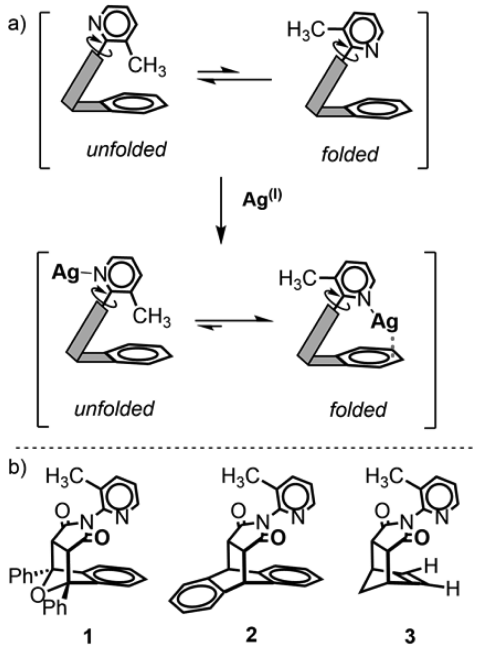

[a](a) Representations of the *folded*–*unfolded* conformational equilibria of the molecular torsion balances that provide a quantitative measure of the intramolecular Ag–π interaction (red broken line) from the comparison of the change of the equilibria in the absence (top) and presence of Ag(I) (bottom). (b) Structures of molecular balances **1** and **2** and control balance **3** (shown in their *folded* conformers).

Received: May 1, 2015
Published: June 12, 2015

DOI: 10.1021/jacs.5b04554
J. Am. Chem. Soc. 2015, 137, 8014–8017

Balances **1** and **2** and control balance **3** were readily synthesized in 1 or 2 steps, using previously described synthetic routes.[16] The crystal structures of **1** and **2** (Figure 1a–c) showed

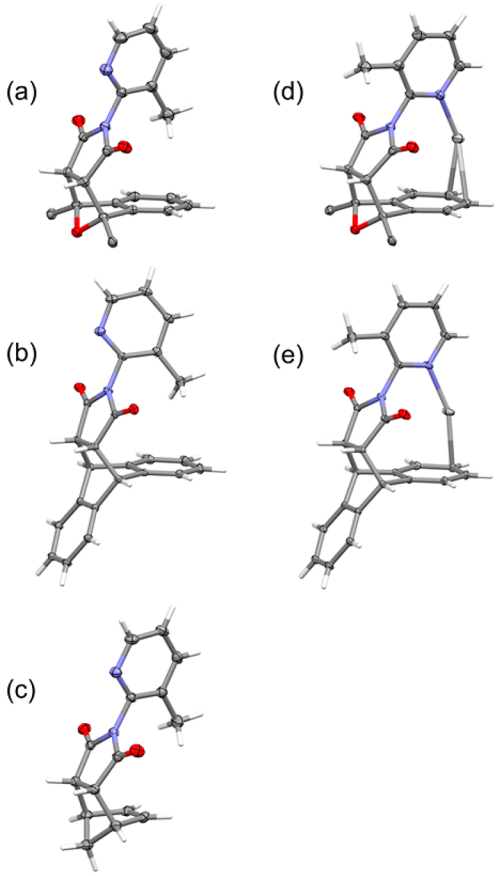

Figure 1. X-ray structures of balances (a) **1**, (b) **2**, and (c) **3** and silver complexes (d) **1·Ag** and (e) **2·Ag**. The bridgehead phenyl groups in **1** and **1·Ag** are hidden for clarity, as well as BF_4 anions and solvent molecules for **1·Ag** and **2·Ag**. For **2·Ag**, only the major η^1 complex (82%) is shown, the structurally similar minor η^2 complex (18%) is not shown.

the expected nonplanar geometry of the *N*-pyridyl and succinimide rings leading to the two distinct conformers.[4a] Both **1** and **2** crystallized exclusively in the *unfolded* conformer with the pyridine nitrogen pointing away from the benzene shelf. The driving force appears to be the formation of an attractive intramolecular CH–π interaction[17] between the *ortho*-methyl group and the benzene shelf.[12b,18] The crystal structure of control balance **3** was nearly structurally identical to **1** and **2**, confirming its viability as a control molecule. The pyridine-rotor of **3** adopted a similar nonplanar geometry and the *endo*-bicyclic framework of **3** was superimposable onto the bicyclic frameworks of **1** and **2**.[19]

Next, the ability of the balances to coordinate and form intramolecular Ag–π interactions was assessed in the solid-state and in solution. Crystal structures of the Ag(I) complexes of **1** and **2** were obtained by cocrystallization with $AgBF_4$ from $MeOH/CH_2Cl_2$ (Figure 1d,e). In the solid-state, **1**·Ag and **2**·Ag were in the *folded* conformation and, more importantly, formed well-defined intramolecular Ag–π interactions. The silver atoms were coordinated to the pyridine nitrogens and formed Ag–π interactions with the outermost edge of the benzene shelves. The η^2 and η^1 coordination geometries in **1·Ag** and **2·Ag** were consistent with the coordination geometries of previous Ag·benzene complexes,[20] with relatively short Ag–C contacts of 2.304 to 2.520 Å.[21] In **1**·Ag, the Ag atom formed an η^2 interaction with the Ag atom almost directly over the center of a C=C bond with similar Ag–C distances of 2.36 and 2.52 Å. In **2**·Ag, the Ag atom was disordered with two similar Ag–π coordination geometries. The major structure (82%) was an η^1 complex where the Ag atom formed one short Ag–C interaction (2.30 Å). The minor structure (18%) was an η^2 complex (not shown) that had a similar Ag–π coordination geometry as the **1·Ag** complex with Ag–C distances of 2.38 and 2.49 Å.

Once the ability of the balances to form Ag–π interactions in the solid-state was established, the Ag–π interactions were characterized in solution by ^{1}H NMR. Specifically, the strengths of the intramolecular interactions were quantitatively measured by their influence on the *folded–unfolded* equilibrium. The methyl group on the pyridine rotor not only served as a "counterweight" for the Ag–π interaction but also slowed the rotation of the *N*-pyridyl rotor to allow measurement by integration of the ^{1}H NMR spectra at room temperature. The *folded–unfolded* ratios and folding energies (ΔG) were measured by integration of the peaks corresponding to the respective conformers with an accuracy of ±0.03 kcal/mol.[22] The formation of the intramolecular Ag–π interactions in balances **1** and **2** was evident from the shift in the folding ratios in favor of the *folded*-conformers upon addition of $AgBF_4$ (Figure 2). The *folded–*

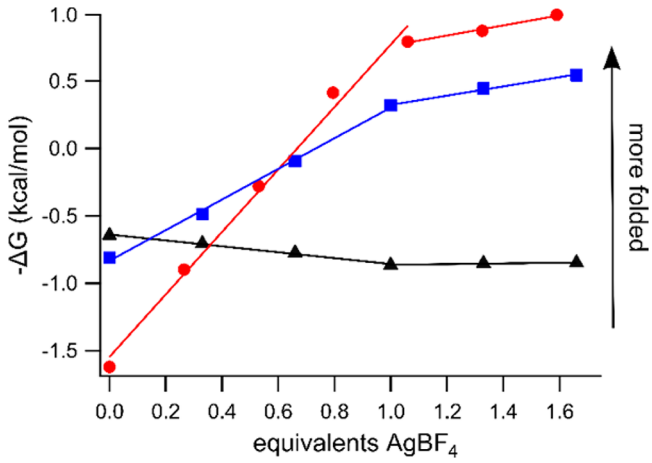

Figure 2. Negative folding energies ($-\Delta G$) of **1**, (■) **2** (●), and **3** (▲) in CD_2Cl_2 (±0.03 kcal/mol) as measured by integration of the ^{1}H NMR spectra (21 °C) versus equivalents of added $AgBF_4$. A solution of $AgBF_4$ (0.45 M) in methanol-d_4 was added incrementally to a solution of molecular balance (0.030 M) in dichloromethane-d_2.

unfolded ratios changed from <1.0 (0.25 and 0.064) in the absence of Ag(I) to >1.0 (1.72 and 3.83) in the presence of 1.0 equiv of $AgBF_4$. By comparison, the addition of $AgBF_4$ to control balance **3**, which cannot form an intramolecular Ag–π interaction, showed only a small change in the *folded–unfolded* ratio in the opposite direction (0.34 to 0.23). The 1:1 (balance to Ag) stoichiometries were confirmed by NMR titrations (Figure 2). A clear break was observed in all three titration curves at 1.0 equiv of added $AgBF_4$. In addition, the expected downfield shifts (+0.05–0.09 ppm) were observed for the pyridyl protons during the titrations due to the coordination of Ag(I) ion to the pyridine nitrogens.

The above analysis provided a measure of the Ag–π interaction energies relative to the CH–π interactions in the

DOI: 10.1021/jacs.5b04554
J. Am. Chem. Soc. 2015, 137, 8014–8017

unfolded conformers. The Ag–π interactions in **1**·Ag and **2**·Ag were stronger than the CH–π interactions as their *folded*–*unfolded* ratios were greater than 1.0. Based on our previous estimates of CH–π interaction energies in this balance system of approximately −1.0 kcal/mol,[12,13] the Ag–π interactions in **1**·Ag and **2**·Ag are slightly stronger than −1.0 kcal/mol.

A more accurate estimate of the Ag–π interaction energy was calculated using a double mutant cycle (DMC) analysis that incorporated the folding energies of control balance **3** and **3**·Ag (Figure 3).[23] The DMC analyses subtracted out the influence of

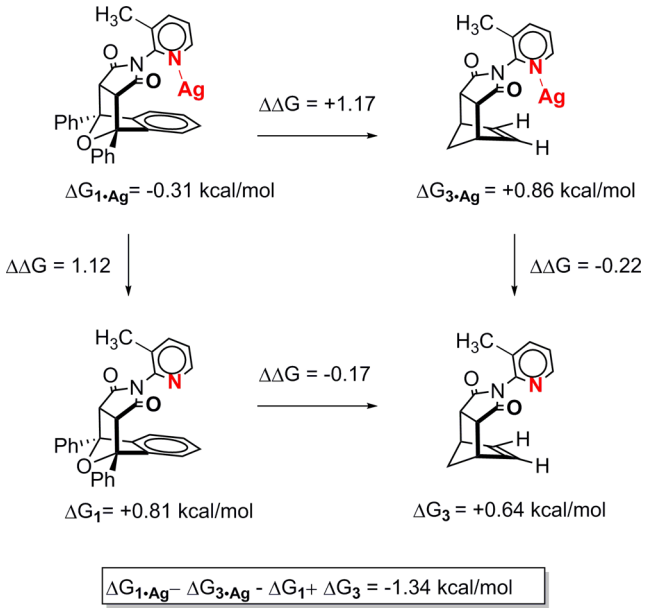

Figure 3. Double mutant cycle analysis for isolating the Ag–π interaction energy in **1**·Ag by subtracting out secondary interactions, CH–π interactions, and dipole effects. A similar DMC analysis was performed for the Ag–π interaction in **2**·**Ag** (not shown) to yield an Ag–π energy of −2.63 kcal/mol.

the CH–π interactions, other secondary interactions, and dipole effects to yield Ag–π interaction energies of −1.34 and −2.63 kcal/mol in **1**·Ag and **2**·Ag, respectively. The magnitude of these interactions is comparable to other noncovalent interactions of charged species such as charge-assisted hydrogen bonds or salt-bridge.[24] The weak nature of this interaction helps explain why systems that utilized Ag–π interactions[8] in solution required multiple Ag–π interactions or additional coordination interactions. It is also consistent with previous measurements of single Ag–π interactions in bimolecular systems, which found either very small (−0.20 kcal/mol) or unfavorable interaction (+0.54 kcal/mol) energies.[8e] The reason is that the weak Ag–π interaction is of comparable magnitude as the translational entropy penalty of metal ligation in these bimolecular systems.[25]

The strengths of the Ag–π interactions in **1**·Ag and **2**·Ag were also measured in different solvent environments and interaction geometries. Not surprisingly, the weak Ag–π interactions were found to be very sensitive to changes in either variable. For example, the difference in the Ag–π interaction energies in **1**·Ag and **2**·Ag was attributed to variations in their Ag–π geometries. The higher Ag–π interaction energy in **2**·Ag was attributed to the larger bite angle that allowed the N–Ag–π bond angle to be closer to the preferred linear geometry.[3e] The N–Ag–π bond angles in the **1**·Ag and **2**·Ag (Figure 4) were 144.8° and 160.7°.[26] These variations in the bite angle are due to the different

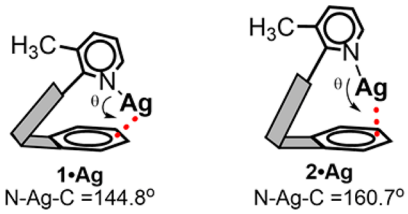

Figure 4. Representations of the different bite-angle geometries in **1**·**Ag** and **2**·**Ag**.

geometric constraints imposed by the −O− and −1,2-arene bridges on the backside of the bicyclic framework.[27] The larger bite angle of **2** is also evident from a comparison of the intramolecular CH–π interaction energies in **1** and **2**. The smaller bite angle in **1** positions the *ortho*-methyl group too close to the benzene shelf leading to repulsive steric interactions and a lower folding energy in **1** (−0.81 vs −1.62 kcal/mol) than in **2**.

Finally, the solvent dependence of the Ag–π interaction in **2**·**Ag** was assessed. The interaction energy was observed to systematically decrease with increasing solvent polarity: methylene chloride (−2.63 kcal/mol), chloroform (−2.47 kcal/mol), acetone (−1.20 kcal/mol), and acetonitrile (0.00 kcal/mol). Thus, in the most polar solvent, acetonitrile, no interaction between the Ag ions and the balances was observed. The acetonitrile outcompetes both the coordinating pyridine and π-ligands of the balances.

In conclusion, a new series of molecular torsion balances were designed to experimentally measure the strength of a single intramolecular Ag–π interaction in solution. The interactions were found to be very weak (−1.34 to −2.63 kcal/mol), which were comparable to noncovalent interactions of charged species. These low interaction energies are consistent with the previously reported difficulties in forming and measuring stability constants for bimolecular complexes held together by single Ag–π interactions. It also corroborates the necessity to incorporate multiple interactions into the design of supramolecular systems that utilize Ag–π interactions. This study also sheds light on how the Ag–π interaction can be easily disrupted by small changes in geometry and solvent environment. One limitation of this study is that the Ag(I) was coordinated to a pyridine nitrogen, which reduced the electrostatic charge on the Ag(I). Thus, the measured Ag–π interaction energy is probably smaller than that of an uncoordinated Ag(I), such as those observed in the gas-phase or in crystal structures. Further studies of other weak metal–π interactions and stability trends are currently underway in our laboratory employing the molecular torsion balance approach.

■ ASSOCIATED CONTENT

Supporting Information

Experimental details, ^{1}H and ^{13}C NMR spectra, X-ray data (CIF), and titration data for balances **1**–**3**. The Supporting Information is available free of charge on the ACS Publications website at DOI: 10.1021/jacs.5b04554.

■ AUTHOR INFORMATION

Corresponding Author

*shimizu@mail.chem.sc.edu

Notes

The authors declare no competing financial interest.

DOI: 10.1021/jacs.5b04554
J. Am. Chem. Soc. 2015, 137, 8014–8017

■ ACKNOWLEDGMENTS

The authors acknowledge the support of the National Science Foundation (CHE 1310139).

■ REFERENCES

(1) (a) Dougherty, D. A. *Science* **1996**, *271*, 163−168. (b) Ma, J. C.; Dougherty, D. A. *Chem. Rev.* **1997**, *97*, 1303−1324. (c) Gokel, G. W. *Chem. Commun.* **2003**, 2847−2852.
(2) Mahadevi, A. S.; Sastry, G. N. *Chem. Rev.* **2013**, *113*, 2100−2138.
(3) (a) Griffith, E. A. H.; Amma, E. L. *J. Am. Chem. Soc.* **1974**, *96*, 743−749. (b) Pierre, J.-L.; Baret, P.; Chautemps, P.; Armand, M. *J. Am. Chem. Soc.* **1981**, *103*, 2986. (c) Dias, H. V. R.; Wang, Z.; Jin, W. *Inorg. Chem.* **1997**, *36*, 6205−6215. (d) Munakata, M.; Wu, L. P.; Ning, G. L. *Coord. Chem. Rev.* **2000**, *198*, 171−203. (e) Lindeman, S. V.; Rathore, R.; Kochi, J. K. *Inorg. Chem.* **2000**, *39*, 5707−5716.
(4) (a) Curran, D. P.; Hongyan, Q.; Geib, S. J.; DeMello, N. C. *J. Am. Chem. Soc.* **1994**, *116*, 3131−3132. (b) Rebek, J., Jr. *Chemtracts: Org. Chem.* **1989**, *2*, 337−352.
(5) (a) Laali, K. K.; Hupertz, S.; Temu, A. G.; Galembeck, S. E. *Org. Biomol. Chem.* **2005**, *3*, 2319−2326. (b) Takino, M.; Daishima, S.; Yamaguchi, K.; Nakahara, T. *J. Chromatogr A* **2001**, *928*, 53−61.
(6) Omoto, K.; Tashiro, S.; Kuritani, M.; Shionoya, M. *J. Am. Chem. Soc.* **2014**, *136*, 17946−17949.
(7) (a) Chebny, V. J.; Rathore, R. *J. Am. Chem. Soc.* **2007**, *129*, 8458−8465. (b) Gao, C.-Y.; Zhao, L.; Wang, M.-X. *J. Am. Chem. Soc.* **2012**, *134*, 824−827. (c) Zang, S.-Q.; Han, J.; Mak, T. C. W. *Organometallics.* **2009**, *28*, 2677−2683. (d) Côté, A. P.; Shimizu, G. K. H. *Inorg. Chem.* **2004**, *43*, 6663−6673.
(8) (a) Rathore, R.; Chebny, V. J.; Abdelwahed, S. H. *J. Am. Chem. Soc.* **2005**, *127*, 8012−8013. (b) Emond, S. J.; Debroy, P.; Rathore, R. *Org. Lett.* **2008**, *10*, 389−392. (c) Habata, Y.; Ikeda, M.; Yamada, S.; Takahashi, H.; Ueno, S.; Suzuki, T.; Kuwahara, S. *Org. Lett.* **2012**, *14*, 4576−4579. (d) Habata, Y.; Taniguchi, A.; Ikeda, M.; Hiraoka, T.; Matsuyama, N.; Otsuka, S.; Kuwahara, S. *Inorg. Chem.* **2013**, *52*, 2542−2549. (e) Gogoll, A.; Polavarapu, P.; Grennberg, H. *Inorg. Chem.* **2007**, *46*, 5271−5275.
(9) Kunze, A.; Balalaie, S.; Gleiter, R.; Rominger, F. *Eur. J. Org. Chem.* **2006**, 2942−2955.
(10) (a) Kumpf, R. A.; Dougherty, D. A. *Science* **1993**, *261*, 1708−1710. (b) Kim, D.; Hu, S.; Tarakeshwar, P.; Kim, K. S.; Lisy, J. M. *J. Phys. Chem. A* **2003**, *107*, 1228−1238.
(11) (a) Paliwal, S.; Geib, S.; Wilcox, C. S. *J. Am. Chem. Soc.* **1994**, *116*, 4497−4498. (b) Mati, I. K.; Cockroft, S. L. *Chem. Soc. Rev.* **2010**, *39*, 4195−4205.
(12) (a) Carrol, W. R.; Zhao, C.; Smith, M. D.; Pellechia, P. J.; Shimizu, K. D. *Org. Lett.* **2011**, *13*, 4320−4323. (b) Li, P.; Parker, T. M.; Hwang, J.; Deng, F.; Smith, M. D.; Pellechia, P. J.; Sherrill, C. D.; Shimizu, K. D. *Org. Lett.* **2014**, *16*, 5064−5067.
(13) Zhao, C.; Parrish, R. M.; Smith, M. D.; Pellechia, P. J.; Sherrill, C. D.; Shimizu, K. D. *J. Am. Chem. Soc.* **2012**, *134*, 14306−14309.
(14) Li, P.; Zhao, C.; Smith, M. D.; Shimizu, K. D. *J. Org. Chem.* **2013**, *78*, 5303−5313.
(15) (a) Carroll, W. R.; Pellechia, P. J.; Shimizu, K. D. *Org. Lett.* **2008**, *10*, 3547−3550. (b) Hwang, J.; Li, P.; Carroll, W. R.; Pellechia, P. J.; Shimizu, K. D. *J. Am. Chem. Soc.* **2014**, *136*, 14060−14067.
(16) (a) Mahanti, S.; Verma, S. M. *Indian J. Chem.* **1982**, *21B*, 1098−1110. (b) Kishikawa, K.; Yoshizaki, K.; Kohmoto, S.; Yamamoto, M.; Yamaguchi, K.; Yamada, K. *J. Chem. Soc., Perkin Trans.* **1997**, *1*, 1233−1239. (c) Grossmann, G.; Potrzebowski, M. J.; Olejniczak, S.; Ziolkowska, N. E.; Bujacz, G. D.; Ciesielski, W.; Prezdo, W.; Nazarov, V.; Golovko, V. *New J. Chem.* **2003**, *27*, 1095−1101. (d) Weber, E.; Finge, S.; Csöregh, I. *J. Org. Chem.* **1991**, *56*, 7281−7288.
(17) (a) Nishio, M. *Phys. Chem. Chem. Phys.* **2011**, *13*, 13873−13900. (b) Takahashi, O.; Kohno, Y.; Nishio, M. *Chem. Rev.* **2010**, *110*, 6049−6076. (c) Nishio, M.; Umezawa, Y.; Honda, K.; Tsuboyama, S.; Suezawa, H. *CrystEngComm* **2009**, *11*, 1757−1788.
(18) Nijamudheen, A.; Jose, D.; Shine, A.; Datta, A. *J. Phys. Chem. Lett.* **2012**, *3*, 1493−1496.
(19) See SI Figure S12 for comparison of balance **1**−**3** crystal structures.
(20) Pérez-Galán, P.; Delpont, N.; Herrero-Gómez, E.; Maseras, F.; Echavarren, A. M. *Chem.—Eur. J.* **2010**, *16*, 5324−5332.
(21) CSD search results found typical Ag−C bond distances range from 2.32 to 3.07 Å. See SI for more information.
(22) For our balance systems, the error in quantitative NMR analysis of the conformational equilibrium in solution at room temperature is typically 1−5% for the conformation ratios between 1/20 and 20/1. This gives a conservative estimate for the error in the calculated folding energy of no higher than ±0.03 kcal/mol. See error analysis in SI for details.
(23) Cockroft, S. L.; Hunter, C. A. *Chem. Soc. Rev.* **2007**, *36*, 172−188.
(24) Pletneva, E. V.; Laederach, A. T.; Fulton, D. B.; Kostic, N. M. *J. Am. Chem. Soc.* **2001**, *123*, 6232−6245.
(25) (a) Bohm, H. J. *J. Comput.-Aided Mol. Des.* **1994**, *8*, 243−356. (b) Hunter, C. A. *Agnew. Chem. Int. Ed.* **2004**, *43*, 5310−5324.
(26) The bite angle for the minor structure was 157.4°.
(27) Bhayana, B.; Arms, M. R. *J. Org. Chem.* **2011**, *76*, 3594−3596.

DOI: 10.1021/jacs.5b04554
J. Am. Chem. Soc. 2015, 137, 8014−8017